Engineering Solid Mechanics 10 (2022) 57-70

Contents lists available at GrowingScience

Engineering Solid Mechanics

homepage: www.GrowingScience.com/esm

Simplified equations for determining double-k fracture parameters of concrete for compact tension test

Rajendra K. Choubey[a*] and Shailendra Kumar[b]

[a]*Associate Professor, Department of Civil Engineering, School of Engineering & Technology, Guru Ghasidas Vishwavidyalaya (A Central University), Bilaspur (C.G.) - 495009, India*
[b]*Professor, Department of Civil Engineering, School of Engineering & Technology, Guru Ghasidas Vishwavidyalaya (A Central University), Bilaspur (C.G.) - 495009, India*

ARTICLEINFO

Article history:
Received 21 June 2021
Accepted 26 November 2021
Available online
27 November 2021

Keywords:
Compact tension test
Double-K fracture parameters
Non dimensional parameters
Concrete
Crack propagation

ABSTRACT

Polynomial equations in non-dimensional form for various fracture parameters of double-K fracture model for compact tension specimen have been derived and presented in this paper. These equations can be used for computing different double-K fracture parameters of concrete for known material properties and specimen size having relative size of initial crack length of 0.3 without involving much complexity in numerical computations. Values of peak load and corresponding crack opening displacement as necessary to compute the double-K fracture parameters of concrete have been derived from the established fictitious crack model in the present study. A simplified equation in non-dimensional form between peak load and critical crack opening displacement as obtained from a fictitious crack model has also been presented.

1. Introduction

Concrete is a quasi-brittle material in which a variable fracture process zone exists ahead of a macro crack during loading. Due to this, the linear elastic fracture mechanics (LEFM) becomes inapplicable directly for the study of crack propagation phenomena in such material. Researchers in the past have developed many nonlinear fracture models such as the fictitious crack model (FCM) or cohesive crack model (CCM) (Carpinteri, 1989; Elices et al., 2009; Hillerborg et al., 1976; Kumar & Barai, 2008b; Kwon et al., 2008; Park et al., 2008; Petersson, 1981; Planas & Elices 1991; Roesler et al., 2007; Zhao et al., 2008), crack band model (CBM) (Bazant & Oh, 1983), two parameter fracture model (TPFM) (Jenq & Shah, 1985), effective crack model (ECM) (Nallathambi & Karihaloo 1986), size effect model (SEM) (Bazant et al., 1986, Akbardoost et al., 2014), K_R-curve method based on cohesive force distribution (Xu & Reinhardt 1998, 1999), double-*K* fracture model (DKFM) (Xu & Reinhardt 1999a,b,c, 2000; Zhao & Xu, 2002; Zhang et al., 2007; Kumar & Barai, 2008, 2009, 2010a,b; Xu & Zhu, 2009; Zhang & Xu, 2011; Hu & Lu, 2012; Hu et al., 2012, 2015; Kumar et al., 2012; Qing & Li 2013; Kumar et al., 2014; Pandey et al., 2016; Choubey et al., 2016, 2017; Qing et al., 2017; Ruiz et al., 2016; Qing et al., 2018; Choubey & Kumar, 2018; Pradhan et al., 2018; Li et al., 2019) and double-*G* fracture model (DGFM) (Xu & Zhang 2008) for crack propagation studies in concrete and concrete structures. The two important material constants (i.e. tensile strength and fracture toughness) are independent of specimen size, geometry or type (Guan et al., 2019).

Initial cracking toughness (K_{IC}^{ini}) and unstable fracture toughness (K_{IC}^{un}) are two material parameters that can characterize the DKFM. Extensive numerical and experimental investigations have been carried out using double-K fracture (DKF)

* Corresponding author.
E-mail addresses: rkchoubey.ggv@gmail.com (R. K. Choubey)

doi: 10.5267/j.esm.2021.10.002

parameters of concrete. Simplified polynomial equations have been developed recently by Choubey and Kumar (2018) for determining the DKF parameter of concrete with variable strengths and material properties, for three-point bend test (TPBT) specimen. The derived equations can predict the DKF Parameter of concrete with negligible error as compared to those obtained based on experimental results. Also, these equations avoid complexities in computations of fracture parameters that were involved in using the existing analytical methods. Rooholamini et al. (2018a,b) and Fakhri et al. (2021) studied the fracture toughness of different concrete materials using edge crack ben beam samples. Hou et al. (2019) solved the cohesive zone model analytic function for concrete based on wedge-splitting tests on a CT specimen and revealed a new method for solving the tensile strain softening curve. In continuation with the previous studies (Choubey and Kumar 2018), the authors in the present study have extended the work for the compact tension (CT) specimen and made an attempt to derive non-dimensional polynomial equations for predicting the DKF parameters of concrete for the given material properties and specimen dimensions. To this end, three different concrete strengths and corresponding material properties for the specimen size range 100-500 mm with initial notch length to depth ratio of 0.3, are considered for the compact tension test. The desired numerical data for determining the DKF parameters are obtained from the developed FCM model for CT specimen. The influence of varying concrete strength on different fracture parameters of DKFM is reported in the present study. Subsequently, all the non-dimensional fracture parameters for varying concrete strength are plotted with respect to specimen size in terms of non-dimensional parameters, and simple polynomial equations have been derived for computing the DKF parameters of CT specimen for the known values of material properties and specimen size.

2. Determination of double-k fracture parameters for CT specimen

The dimensions and configuration of standard CT specimen according to the ASTM standard E-399 (2006) (Karihaloo and Nallathambi 1991) are shown in Fig.1 in which D_1=1.25D, H=0.6D, H_1=0.275D.

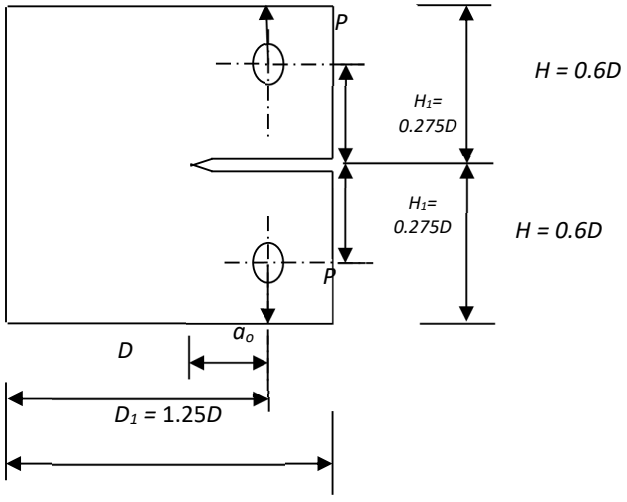

Fig. 1. Dimensions and loading schemes of CT specimen

2.1 Determination of effective crack extension

During the crack propagation, to determine the effective crack extension value, a *priori*, the P-COD plot for the CT geometry is to be known. Using linear asymptotic superposition assumption (Xu & Reinhardt, 1999), the equivalent-elastic crack length a_c corresponding to maximum load P_u for standard CT specimen is solved using LEFM equations (Murakami, 1987). Hence, the COD is expressed as:

$$COD = \frac{P}{BE} V_1(\alpha) \tag{1}$$

$$V_1(\alpha) = \left[2.163 + 12.219\alpha - 20.065\alpha^2 - 0.9925\alpha^3 + 20.609\alpha^4 - 9.9314\alpha^5 \right] \left(\frac{1+\alpha}{1-\alpha} \right)^2 \tag{2}$$

where, $\alpha = \frac{a}{D}$, $a = a_c$ equivalent-elastic crack length at maximum load P_u, the empirical Eq. (2) is valid within 0.5% accuracy for $0.2 \leq \alpha \leq 0.975$. The value E is calculated using the P-COD curve as:

$$E = \frac{V_1(\alpha_o)}{C_i B} \tag{3}$$

where, E is modulus of elasticity of concrete. Here, the value of E determined using compressive cylinder tests is used to obtain the critical crack length of the specimen (ASTM International Standard E399-06, 2006).

2.2 Computation of K_{IC}^{un} and K_{IC}^{ini}

In the fictitious crack zone, a linearly varying cohesive stress distribution is assumed, which gives rise to cohesion toughness as a part of total toughness of the cracked body. At the tip of effective crack length, the total stress intensity factor (SIF) "K_I" is equal to the sum of SIF caused due to external load K_I^P and SIF contributed by cohesive stress K_I^C as shown in Fig. 2 That is:

$$K_I = K_I^P + K_I^C \tag{4}$$

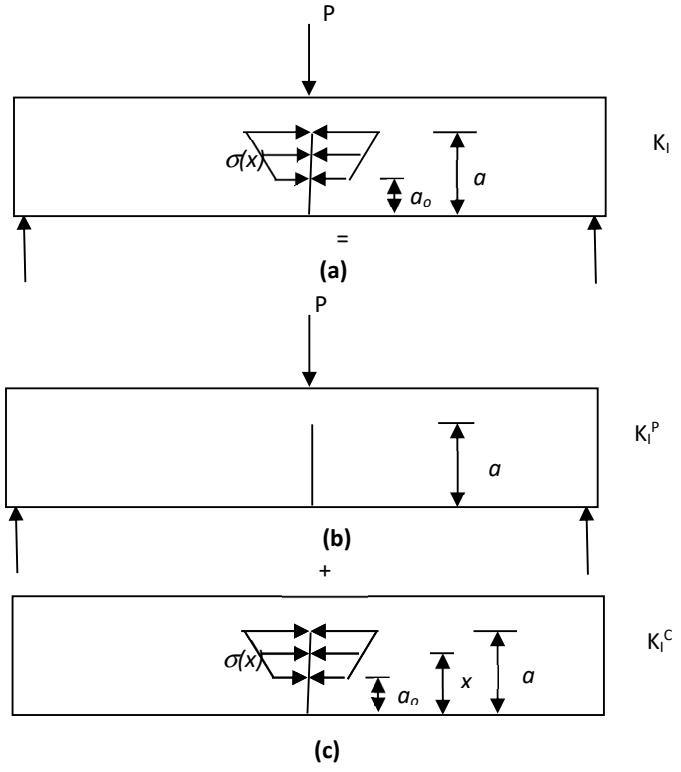

Fig. 2. Calculation of SIF using superposition method

After determining the critical effective crack extension at unstable condition of loading, the two parameters, initiation toughness (K_{IC}^{ini}) and unstable fracture toughness (K_{IC}^{un}) of DKFM is determined using LEFM formulae as given in the following equations. The SIF is expressed as:

$$K_I = \sigma_N \sqrt{D} k(\alpha) \tag{5}$$

where, $k(\alpha)$ is a geometric factor, $\alpha = a/D$ and σ_N is the nominal stress. The SIF for standard CT specimen is determined using Eq. (5) for the following values of σ_N and $k(\alpha)$ (Karihaloo and Nallathambi 1991)

$$\sigma_N = \frac{P}{BD} \tag{6}$$

$$k(\alpha) = \frac{(2+\alpha)\left[0.886 + 4.64\alpha - 13.32\alpha^2 + 14.72\alpha^3 - 5.6\alpha^4\right]}{(1-\alpha)^{3/2}} \tag{7}$$

Eq. (7) is valid for $0.2 \le \alpha \le 1$ within 0.5 % accuracy. Above equations can be used in calculation of K_{IC}^{un} at the tip of effective crack length a_c in which $a = a_c$ and $P = P_u$. The K_{IC}^{ini} is calculated using the following inverse relation.

$$K_{IC}^{ini} = K_{IC}^{un} - K_{IC}^{C} \tag{8}$$

In Eq. (8), the value of K_{IC}^{C} using five terms weight function (Kumar and Barai 2009c; 2010a) is expressed in the following form.

$$K_{IC}^{C} = \frac{2}{\sqrt{2\pi a}}\left\{ A_1 a\left[2s^{1/2} + M_1 s + \frac{2}{3}M_2 s^{3/2} + \frac{M_3}{2}s^2 + \frac{2}{5}M_4 s^{5/2} \right] + A_2 a^2\left[\frac{4}{3}s^{3/2} + \frac{M_1}{2}s^2 + \frac{4}{15}M_2 s^{5/2} + \frac{4}{35}M_4 s^{7/2} + \frac{M_3}{6}\left\{1-(a_o/a)^3 - 3sa_o/a\right\}\right]\right\} \tag{9}$$

where, $A_1 = \sigma_s(CTOD_c)$, $A_2 = \dfrac{f_t - \sigma_s(CTOD_c)}{a - a_o}$ and $s = (1 - a_o/a)$, also $a = a_c$ at $P = P_u$. After determining the value of K_{IC}^{C} using Eq. (9), K_{IC}^{ini} can be evaluated using Eq. (8). In which, crack tip opening displacement (CTOD) at critical load (P_u) becomes critical crack tip opening displacement, $CTOD_c$ which is determined using the following expression (Jenq and Shah 1985)

$$CTOD_c = CMOD_c\left\{(1-a_o/a_c)^2 + (1.081 - 1.149a_c/D)[a_o/a_c - (a_o/a_c)^2]\right\}^{1/2} \tag{10}$$

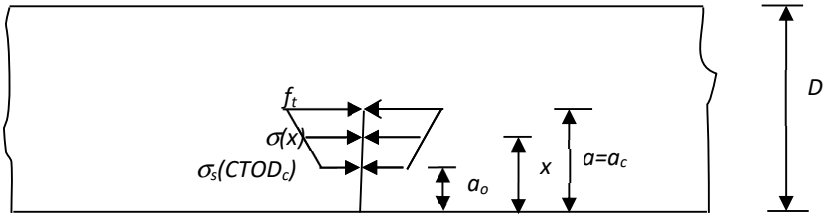

Fig. 3 Distribution of cohesive stress in the fictitious crack zone at critical load.

In which CODc is the crack opening displacement at critical or peak load. The linearly varying distribution of cohesive stress is presented in Fig. 3. In Fig. 3 $\sigma_s(CTOD_c)$ is cohesive stress at the tip of initial notch and cohesive stress distribution $\sigma(x)$ is expressed as:

$$\sigma(x) = \sigma_s(CTOD_c) + \frac{x - a_o}{a - a_o}[f_t - \sigma_s(CTOD_c)] \quad \text{for } 0 \le \text{CTOD} \le C\text{TOD}_c \tag{11}$$

The value of $\sigma_s(CTOD_c)$ is calculated by using softening functions of concrete. In the present work, the nonlinear softening function is used in the computation. This softening function is characterized as:

$$\sigma(w) = f_t\left\{\left[1 + \left(\frac{c_1 w}{w_c}\right)^3\right]\exp\left(\frac{-c_2 w}{w_c}\right) - \frac{w}{w_c}\left(1 + c_1^3\right)\exp\left(-c_2\right)\right\} \tag{12}$$

The value of total fracture energy of concrete G_F is expressed as:

$$G_F = w_c f_t\left\{\frac{1}{c_2}\left[1 + 6\left(\frac{c_1}{c_2}\right)^3\right] - \left[1 + c_1^3\left(1 + \frac{3}{c_2} + \frac{6}{c_2^2} + \frac{6}{c_2^3}\right)\right]\frac{\exp(-c_2)}{c_2} - \left(\frac{1 + c_1^3}{2}\right)\exp(-c_2)\right\} \tag{13}$$

in which, $\sigma(w)$ is the cohesive stress at crack opening displacement w and c_1 and c_2 are the material constants. The w_c is the maximum crack opening displacement at which the cohesive stress becomes zero. For normal concrete the values of c_1 and c_2 are taken as 3 and 7, respectively.

Also the five term weight function $m(x,a)$ of Eq. (9) can be expressed as per equation

$$m(x,a) = \frac{2}{\sqrt{2\pi(a-x)}}\left[1 + M_1(1-x/a)^{1/2} + M_2(1-x/a) + M_3(1-x/a)^{3/2} + M_4(1-x/a)^2\right] \tag{14}$$

The parameters of Eq. (14) that is M_1, M_2, M_3 and M_4 for edge cracks in a finite width of plate subjected to pair of normal forces can be determined using Eqs. (15) and (16) (Kumar and Barai 2009c; 2010a).

$$M_i = \frac{1}{(1-a/D)^{3/2}}\left[a_i + b_i a/D + c_i(a/D)^2 + d_i(a/D)^3 + e_i(a/D)^4 + f_i(a/D)^5\right] \quad (15)$$

for, i = 1 and 3

$$M_i = \left[a_i + b_i a/D\right] \quad (16)$$

for i = 2 and 4

The values of coefficients a_i, b_i, c_i, . . ., f_i of these parameters M_1, M_2, M_3 and M_4 are presented in Table 1.

Table 1. Coefficients of 5 terms weight function parameters M1, M2, M3 and M4 (Kumar and Barai 2009c; 2010a).

i	a_i	b_i	c_i	d_i	e_i	f_i
1	-0.000824975	0.6878602	0.4942668	-3.25418434	3.4426983	-1.3689673
2	0.782308	-3.0488836	-	-	-	-
3	-0.3049218	13.4186519	-23.31662697	35.51066606	-34.440981408	14.10339412
4	0.28347699	-7.378355423	-	-	-	-

Thus, the value of K_{IC}^{C} and K_{IC}^{ini} are determined using Eq. (9) & Eq. (8), respectively

2.3 Fictitious crack model and material properties

Hillerborg and coworkers initially applied FCM or CCM to simulate the softening damage of concrete structures. In the past, the cohesive crack method became popular and was modified and used by many researchers (Petersson 1981; Carpinteri 1989; Planas and Elices 1991; Roesler et al. 2007; Park et al. 2008; Zhao et al. 2008; Kwon et al. 2008; Elices et al. 2009; Kumar and Barai 2008b, 2009c) to show the applications of CCM for characterizing the softening functions and predicting the nonlinear fracture characteristics of concrete using various test configurations.

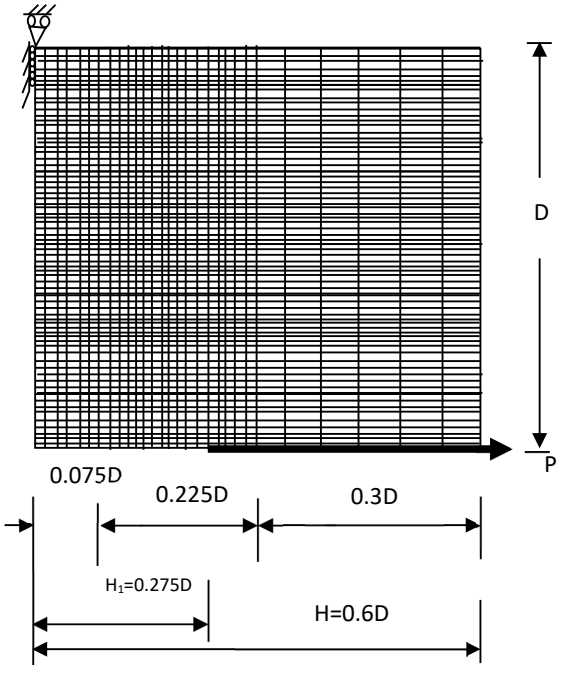

Fig. 4 Finite element mesh for half of the CT specimen

Three material properties (modulus of elasticity E, uniaxial tensile strength (f_t), and fracture energy (G_F)) are required to model FCM or CCM. The FCM for the CT specimens as presented by the authors, Kumar and Barai (2008b, 2009a), is used in the present study. Here, along the potential fracture, the governing equation of the crack opening displacement (COD) line is written. Linear elastic finite element method is determined using the influence coefficients of the COD equation. In finite element calculation, the 4-noded iso-parametric plane elements are used and the COD vector is partitioned according to the enhanced algorithm introduced by Planas and Elices (1991). Consequently, the system of nonlinear simultaneous equations is developed and solved using Newton-Raphson method. For standard CT specimens having size range D = 100-500 mm and

with B = 100 mm, the finite element analysis is carried out, for which due to symmetry, the half of the specimens are discretized as shown in Fig. 4. Total 80 numbers of equal iso-parametric plane elements along the dimension D are considered.

For three concrete mixes (M_1, M_2 and M_3) with Poisson's ratio ν = 0.18 and maximum aggregate size d_a=16 mm are considered in the present study. The material properties for the concrete mixes are considered as per the CEB-FIP Model Code (CEB-Comite Euro-International du Beton-CEB-FIP Model Code 1990) as given in Table 2.

Table 2. Material properties for the concrete mixes as per CEB-FIP Model Code (CEB-Comite Euro-International du Beton-CEB-FIP Model Code 1990)

Concrete Mix	Cylinder characteristic strength, f_{ck} (MPa)	f_t (MPa)	E (GPa)	G_F (N/m)
M_1	20	2.2	26	60
M_2	40	3.5	31	90
M_3	60	4.6	35	115

For simulating FCM in the present investigation, the nonlinear softening function with c_1=3 and c_2=7, respectively is used, for all concrete mixes. In order to obtain non-dimensional fracture parameters, two relations of FCM i.e., characteristic length $l_{ch}=EG_F/f_t^2$ and critical value of stress intensity factor $K_{IC}=\sqrt{(G_F E)}$ are used.

3. Results and discussion

P-COD curves for each size of specimen (D=100, 200, 300, 400 and 500 mm with B=100 mm and a_0/D=0.30) are simulated from FCM. Typical results of P-COD for the CT test for specimen depth of 100 mm and 500 mm at a_o/D ratio of 0.3 are shown in Figs. 5 and 6, respectively. The type of specimen geometry, concrete mix and specimen size are denoted by the legends of Figs. 5-6. For example, CT-M_1-D_1 in Fig.5 denotes the CT specimen made of concrete mix M_1 and specimen size of 100 mm.

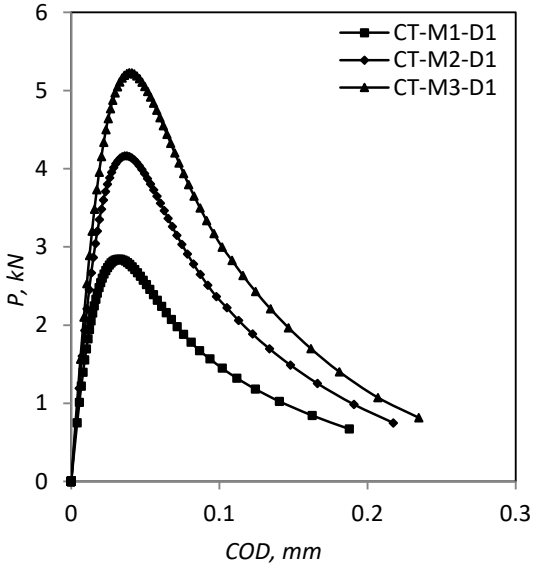

Fig. 5 P-COD curve for specimen depth 100 mm of CT test

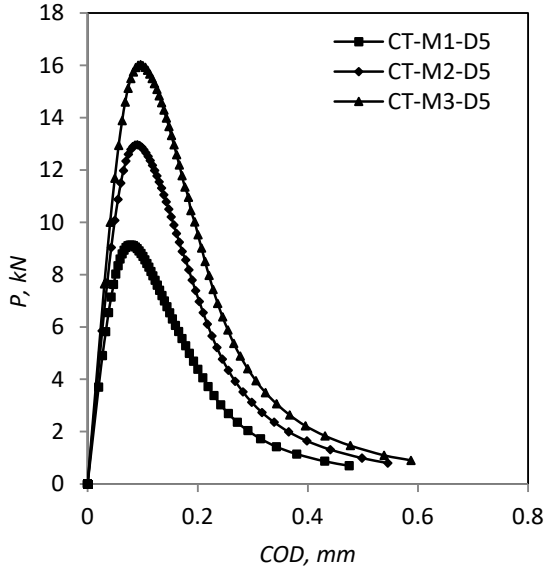

Fig. 6 P-COD curve for specimen depth 500 mm of CT test

In Fig. 8, a non-dimensional parameter $f_t l_{ch}^2/P_u$ is taken on Y-axis and a non-dimensional parameter l_{ch}/COD_c is kept on X-axis. From the plot, it is observed that all the points lie on a straight line which is independent of specimen size. This observation seems to be a true material property that the peak load can be obtained for a given value of critical value of crack opening displacement and material properties of concrete. Hence, the parameter $f_t l_{ch}^2/P_u$ termed as a peak load ratio depends on the material properties and specimen geometry for a given value of geometrical factor a_o/D ratio. Following form of equations representing the non-dimensional peak load ratios can be obtained from linear regressions for the CT specimen.

$$\frac{f_t l_{ch}^2}{P_u} = 0.0086\frac{l_{ch}}{COD_c} - 8.7531 \tag{17}$$

for which, R^2 = 0.993

Eq. (17) can be useful to calculate the P_u for a given COD_c for variable values of concrete strength, E and G_F of concrete for the CT specimen. These equations are valid for nonlinear softening function and a_o/D ratio of 0.3.

Further, the computed values of K_{IC}^{un}, K_{IC}^{C}, K_{IC}^{ini}, P_{ini} and $CTOD_c$ are plotted with respect to tensile strength of concrete for all the specimens through Figs. 9-13, respectively. From the figures, the following observations are made.

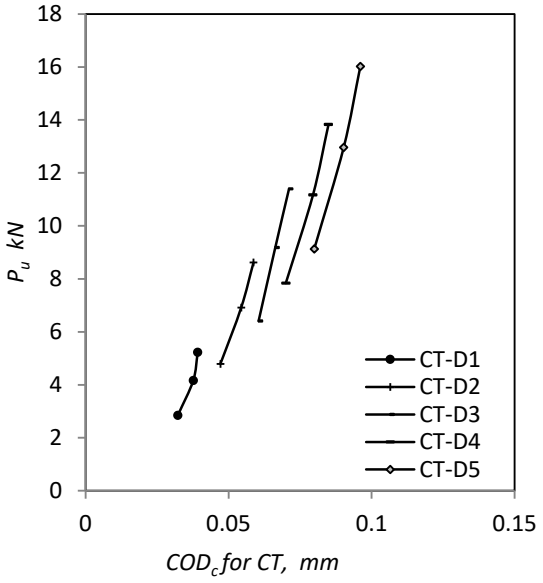

Fig. 7 Relationship between unstable peak load and corresponding COD_c

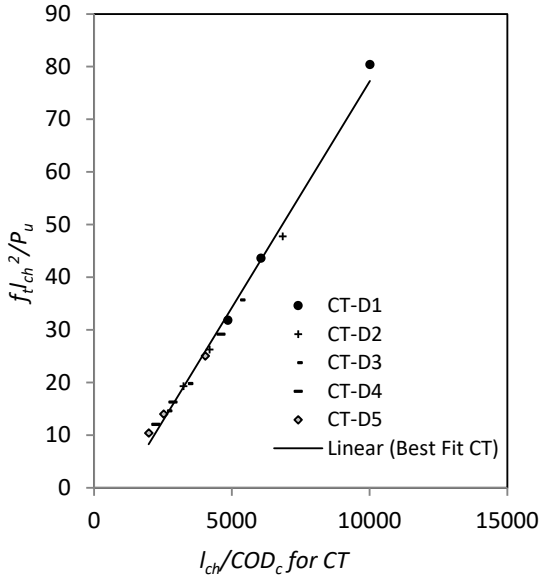

Fig. 8 Relationship between non-dimensional peak load and corresponding COD_c

- It is seen from Fig. 9 that the value of K_{IC}^{un} increases with tensile strength of concrete for a given specimen size and it also increases with increase in specimen size for particular value of concrete strength.
- Fig. 10 shows a similar behavior of K_{IC}^{C} as in case of K_{IC}^{un} that is value of K_{IC}^{C} increases with tensile strength of concrete and it also increases with increase in specimen size for a specified value of concrete strength.
- The observed behavior of K_{IC}^{ini} is different than those of K_{IC}^{un} and K_{IC}^{C} as seen from Fig.11. The value of K_{IC}^{ini} increases with tensile strength of concrete for a given specimen size whereas it decreases with increase in specimen size for a specified value of concrete strength.

The crack initiation load P_{ini} is difficult to measure from the experiments. However, it can be easily determined using inverse method in double-*K* fracture model. Fig. 12 shows the variation of computed value *of* P_{ini} with respect to tensile strength of concrete for both the test geometries. It is observed that the value of P_{ini} increases with increase in tensile strength of concrete for a given specimen size and also it increases with increase in specimen size for a specified value of concrete strength.

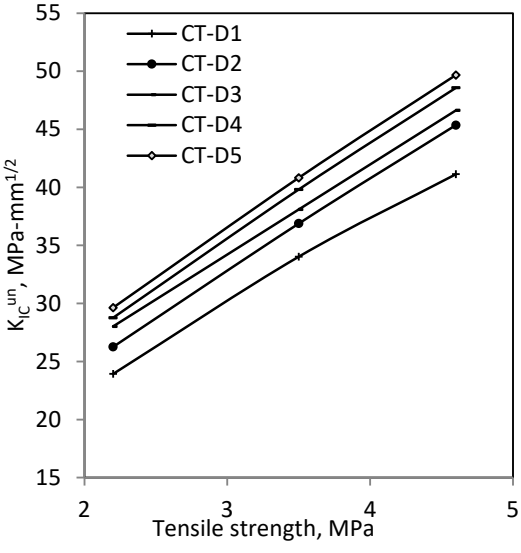

Fig. 9 Influence of tensile strength of concrete on the K_{IC}^{un}

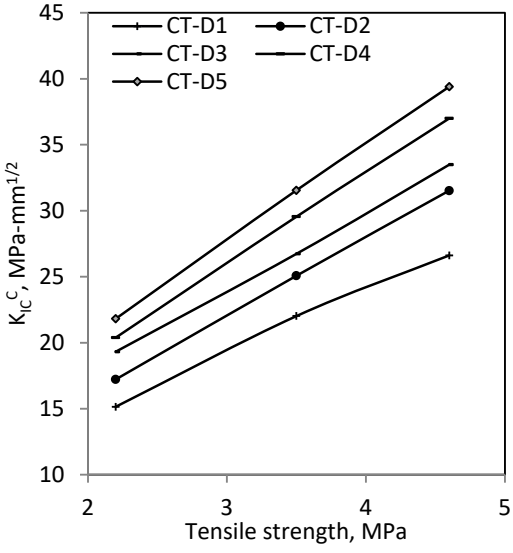

Fig. 10 Influence of tensile strength of concrete on the K_{IC}^{C}

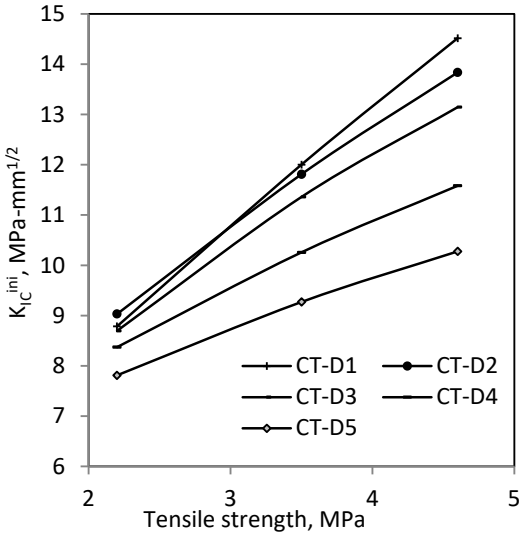

Fig. 11 Influence of tensile strength of concrete on the K_{IC}^{ini}

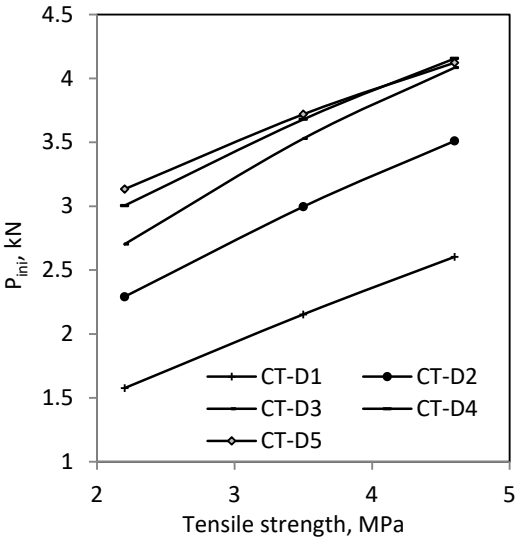

Fig. 12 Influence of tensile strength of concrete on the P_{ini}

- As seen from Fig. 13, the $CTOD_c$ is influenced by specimen size and concrete strength. It is observed that the value of $CTOD_c$ increases with tensile strength of concrete for a given specimen size and also it increases with increase in specimen size for a specified value of concrete strength.
- The ratio of crack initiation load to unstable fracture load (Pini/Pu) is an important parameter which is plotted with respect to tensile strength of concrete as shown in Fig. 14.

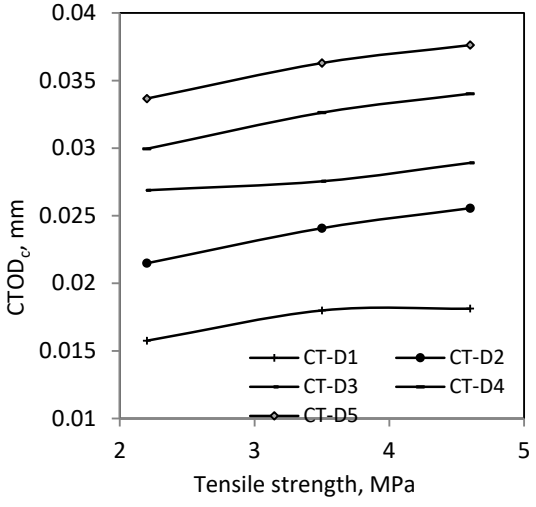

Fig. 13 Influence of tensile strength of concrete on the $CTOD^c$

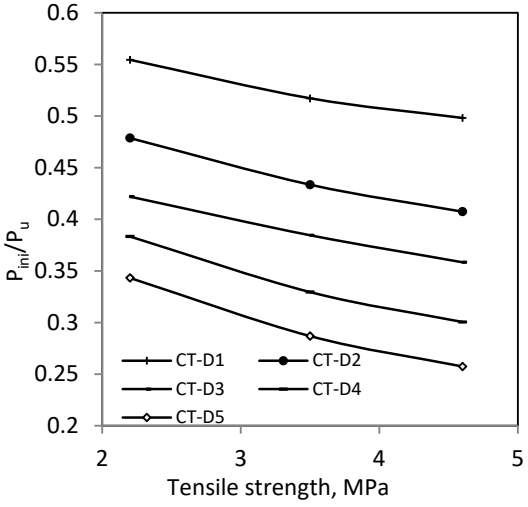

Fig. 14 Variation of P_{ini}/P_u with the tensile strength of concrete

- From the figure it is observed that the ratio (P_{ini}/P_u) depends on the specimen size and concrete strength. The value of P_{ini}/P_u decreases with increase in tensile strength of concrete for a given specimen size and also it decreases with increase in specimen size for a specified value of concrete strength. The calculated values of P_{ini}/P_u for D=100 mm is 0.554, 0.517 and 0.498 for concrete grades M_1, M_2 and M_3 respectively for the CT specimen. Similarly, for D = 500mm, the values of P_{ini}/P_u are 0.343, 0.287 and 0.257 for concrete grades M_1, M_2 and M_3 respectively.

Further, the non-dimensional form of fracture parameters involved in double-K fracture model are plotted with l_{ch}/D ratio and some interesting trends are observed from these plots. The parameter K_{IC}/K_{IC}^{un} for the CT specimen at a_o/D ratio 0.3 is plotted in Fig. 15. It is seen from the figure that the unstable fracture toughness of material increases with the specimen size. The non-dimensional material fracture parameter K_{IC}/K_{IC}^{un} shows a definite relationship with l_{ch}/D ratio for all the three concrete mixes that means this parameter is independent of the concrete strength and its material property. A generalized size-effect relationship for different concrete mixes is obtained for the CT specimen from polynomial regression analysis as given below.

$$\frac{K_{IC}}{K_{IC}^{un}} = 0.0141\left(\frac{l_{ch}}{D}\right)^3 - 0.1208\left(\frac{l_{ch}}{D}\right)^2 + 0.3351\left(\frac{l_{ch}}{D}\right) + 1.1668 \tag{18}$$

for which, $R^2 = 0.991$

Eq. (18) needs only the material properties and specimen size for laboratory size specimens to evaluate the unstable fracture toughness of concrete. The cohesive toughness in non-dimensional parameter K_{IC}/K_{IC}^{C} is plotted with l_{ch}/D ratio as shown in Fig.16. It is observed from the figure that the K_{IC}/K_{IC}^{C} also shows a definite relationship with the l_{ch}/D ratio. The value of cohesive toughness of the material increases with increase in specimen size. For CT, a generalized polynomial regression equation can be obtained and presented as given in Eq. (19).

$$\frac{K_{IC}}{K_{IC}^{C}} = -0.0093\left(\frac{l_{ch}}{D}\right)^4 + 0.1249\left(\frac{l_{ch}}{D}\right)^3 - 0.5804\left(\frac{l_{ch}}{D}\right)^2 + 1.3204\left(\frac{l_{ch}}{D}\right) + 1.1997 \tag{19}$$

for which, $R^2 = 0.998$

Similar to the unstable fracture toughness, one can obtain the value of cohesive toughness of concrete for any concrete strength and given material properties which only depends on specimen size for the CT specimen.

$$\frac{P_{ini}}{P_u} = -0.0095\left(\frac{l_{ch}}{D}\right)^6 + 0.1135\left(\frac{l_{ch}}{D}\right)^5 - 0.5443\left(\frac{l_{ch}}{D}\right)^4 + 1.3414\left(\frac{l_{ch}}{D}\right)^3 - 1.8299\left(\frac{l_{ch}}{D}\right)^2 + 1.4309\left(\frac{l_{ch}}{D}\right) - 0.087 \tag{22}$$

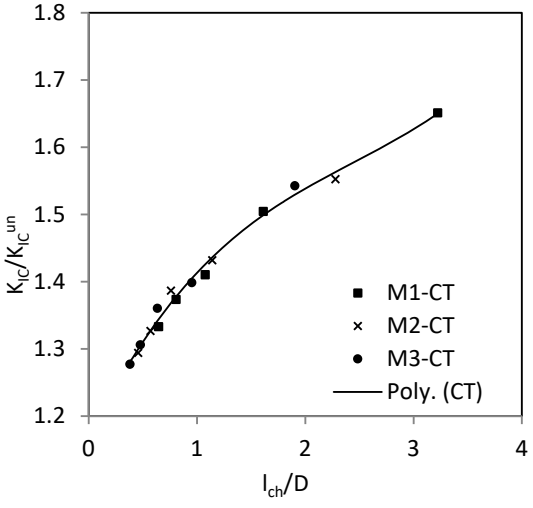

Fig. 15 Variation of unstable fracture toughness with specimen size

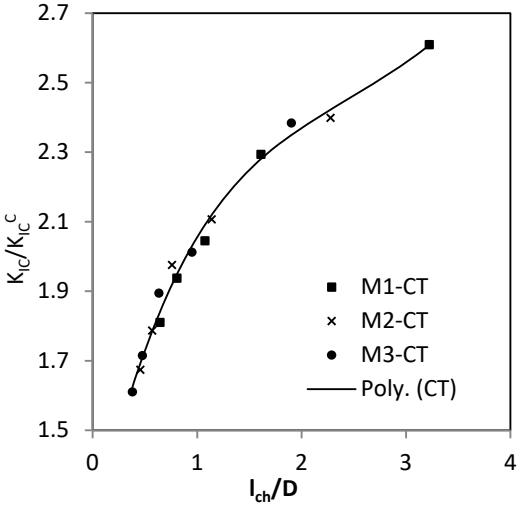

Fig. 16 Variation of cohesive fracture toughness with specimen size

The variation of non-dimensional parameter K_{IC}^{ini}/K_{IC} with l_{ch}/D is shown in Fig. 17 for the CT specimen geometry. It is seen from the figure that a definite relationship between initial cracking toughness and the l_{ch}/D ratio exists. The value of initial cracking toughness of concrete decreases with the increase in specimen size beyond the specimen size 300mm and it is almost constant up to the specimen size of 300 mm. For the CT specimen geometry, a generalized polynomial regression equation can be determined and presented in Eq. (20).

$$\frac{K_{IC}^{ini}}{K_{IC}} = -0.0076\left(\frac{l_{ch}}{D}\right)^6 + 0.0875\left(\frac{l_{ch}}{D}\right)^5 - 0.4022\left(\frac{l_{ch}}{D}\right)^4 + 0.9516\left(\frac{l_{ch}}{D}\right)^3 - 1.2365\left(\frac{l_{ch}}{D}\right)^2 + 0.858\left(\frac{l_{ch}}{D}\right) - 0.0309 \tag{20}$$

for which, $R^2 = 0.986$

Eq. (20) can be used to accurately determine the value of initial cracking toughness for given material properties and specimen depth for the CT test geometry.

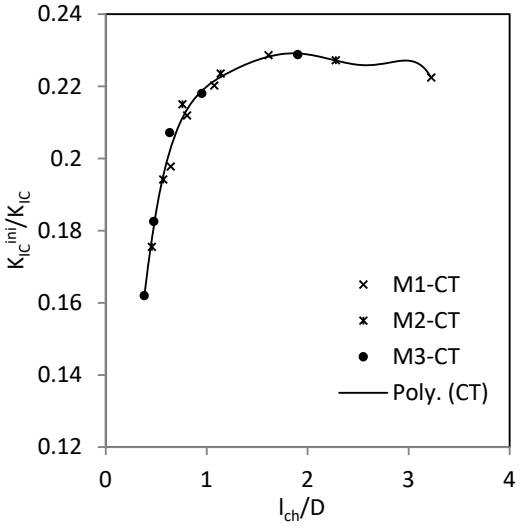

Fig. 17 Variation of initial cracking toughness with specimen size

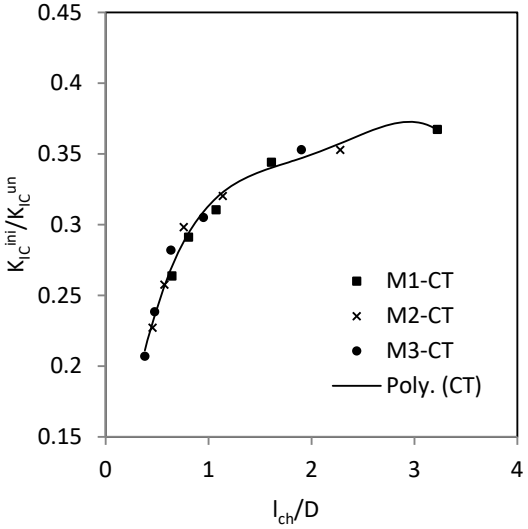

Fig. 18 Variation of K_{IC}^{ini}/K_{IC}^{un} with specimen size

The ratio of K_{IC}^{ini}/K_{IC}^{un} is plotted with the l_{ch}/D ratio in Fig. 18 which also shows a definite relationship between the parameter K_{IC}^{ini}/K_{IC}^{un} and the specimen size in non-dimensional form l_{ch}/D. It is observed that the value of K_{IC}^{ini}/K_{IC}^{un} ratio decreases as the specimen size increases. For D = 100 mm size specimen, the calculated values of K_{IC}^{ini}/K_{IC}^{un} are 0.3672, 0.3528 and 0.3529 for concrete grades M_1, M_2 and M_3 respectively. Similarly, for D = 500 mm, the values of K_{IC}^{ini}/K_{IC}^{un} are 0.2367, 0.2271 and 0.2069 for concrete grades M_1, M_2 and M_3. The values of K_{IC}^{ini}/K_{IC}^{un} as determined from polynomial regression is presented in Eq. (21) for the CT specimen.

$$\frac{K_{IC}^{ini}}{K_{IC}^{un}} = -0.0151\left(\frac{l_{ch}}{D}\right)^4 + 0.1241\left(\frac{l_{ch}}{D}\right)^3 - 0.3745\left(\frac{l_{ch}}{D}\right)^2 + 0.5169\left(\frac{l_{ch}}{D}\right) + 0.0621 \quad (21)$$

for which, $R^2 = 0.983$

For given values of material properties and specimen size the ratio of K_{IC}^{ini}/K_{IC}^{un} can be determined using Eq. (21) for the CT specimen. Also, the ratio of P_{ini}/P_u is plotted with l_{ch}/D ratio for the CT specimen as shown in Fig. 19. From the figure it is observed that the ratio of crack initiation load to the peak load on the structures has a definite relationship with the specimen size *i.e.* l_{ch}/D ratio. This ratio decreases with the increase in the specimen size. The polynomial regression equations as obtained for the CT specimen are presented in Eq. (22).

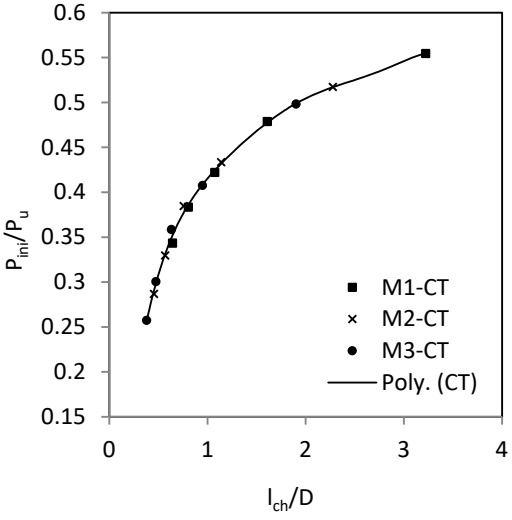

Fig. 19 Variation of P_{ini}/P_u with specimen size

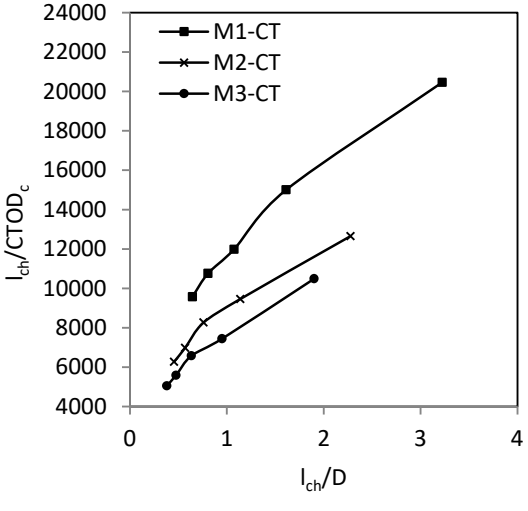

Fig. 20 Variation of $CTOD_c$ with the specimen size

The P_{ini}/P_u ratio for the CT test can be determined using Eq. (22) when material properties of concrete and size of specimen are known. The $CTOD_c$ in terms of non-dimensional form $l_{ch}/CTOD_c$ is plotted with respect to l_{ch}/D as shown in Fig. 20. From the figure it is observed that $CTOD_c$ increases with increase in specimen size and it is different for different grades of concrete materials. It is difficult to obtain a definite relationship between $CTOD_c$ with respect to specimen size for given material properties because the $CTOD_c$ also increases with increase in concrete strength. When the $CTOD_c$ in terms of non-dimensional form $l_{ch}/CTOD_c$ is plotted with respected to l_{ch}/COD_c for the CT specimen as shown in Fig.21, a definite relationship between $CTOD_c$ and COD_c is obtained. It is observed that $l_{ch}/CTOD_c$ varies almost linearly with l_{ch}/COD_c for given fracture material properties. The linear regression equations are obtained and presented in Eq. (23)) for the CT specimen. Eq. (23) can be directly used for determining the $CTOD_c$ for a given value of COD_c for the CT specimen. The derived equations based on non-dimensional parameters for the CT specimen follow the pattern identical to the equations derived and presented by the authors for three-point bending test.

$$\frac{l_{ch}}{CTOD_c} = 1.9217\frac{l_{ch}}{COD_c} + 1459 \tag{23}$$

for which, $R^2 = 0.995$

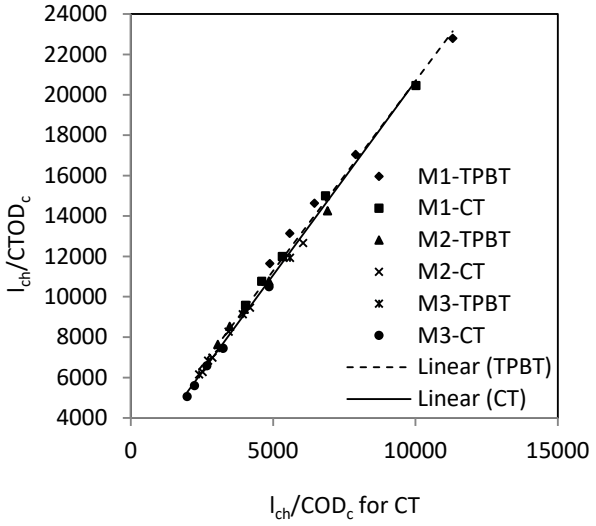

Fig. 21 Relationship between non-dimensional parameters of $CTOD_c$ and COD

4. Conclusions

The effect of varying material properties of concrete on the different fracture parameters of double-K model during compact tension test specimen for size range $100 \le D \le 500$ mm at constant initial crack length to depth ratio of 0.3 was studied and reported in the paper. The following conclusions can be drawn from the present study.

- Peak load and critical crack opening displacement in the non-dimensional forms for the CT specimen geometries maintain a linear relationship. The non-dimensional parameters are independent of specimen size. Simple regression equation is developed and presented for evaluating the peak load for given values of material properties and critical crack opening displacement.
- Parameters like unstable fracture toughness, cohesive toughness, initial cracking toughness, initial cracking load and critical crack-tip opening displacement are influenced by concrete strength and these parameters have linear increasing relationship with concrete strength.
- The derived polynomial equations for CT specimen can be applied for computing different parameters of double-*K* fracture model for known material properties and specimen size. Application of such equations will enable to determine different fracture parameters for CT specimen without involving complexities in computation.
- In the future, the derived equations as presented for the CT specimen in this study as well as for TPBT specimen in the previous study by Choubey and Kumar (2018), can be modified and redeveloped based on extensive experimental results, so that a readymade solution can be prepared in non-dimensional forms for simplified computation of peak load and corresponding crack opening displacement for different parameters of double-K fracture of concrete.

References

Akbardoost, J., Ayatollahi, M. R., Aliha, M. R. M., Pavier, M. J., & Smith, D. J. (2014). Size-dependent fracture behavior of Guiting limestone under mixed mode loading. *International Journal of Rock Mechanics and Mining Sciences, 71*, 369-380.

ASTM International Standard E399-06 (2006) Standard Test Method for Linear-Elastic Method Plane-Strain Fracture Toughness KIC of Metallic Materials. Copyright ASTM International, West Conshohocken, U.S., 1-32.

Bažant, Z.P., & Oh, B.H. (1983). Crack band theory for fracture of concrete. *Materials and Structures, 16*(93), 155–177.

Bažant, Z.P., Kim, J.K., & Pfeiffer, P.A. (1986). Determination of fracture properties from size effect tests. *Journal of Structural Engineering, ASCE, 112*(2), 289-307.

Carpinteri, A. (1989). Cusp catastrophe interpretation of fracture instability. *Journal of the Mechanics and Physics of Solids, 37*(5), 567-582.

CEB-Comite Euro-International du Beton-CEB-FIP Model Code (1990). Bulletin D'Information, EPF Lausanne.

Choubey, R.K., & Kumar, S. (2018). Simplified equations for determining double-k fracture parameters of concrete for 3-point bending test. *Fatigue & Fracture of Engineering Materials & Structures, 4*, 1615-1626.

Choubey, R.K., Kumar, S., & Rao, M.C. (2016). Modeling of fracture parameters for crack propagation in recycled aggregate concrete. *Construction and Building materials, 106*, 168-178.

Choubey, R.K., Kumar, S., & Rao, M.C. (2017). Numerical evaluation of simplified extreme peak load method for determining the double–K fracture parameters of concrete. *International Journal of Engineering & Technology, 9*(3), 2097-2110.

Elices, M., Rocco, C., & Roselló, C. (2009). Cohesive crack modeling of a simple concrete: Experimental and numerical results. *Engineering Fracture Mechanics, 76*, 1398-1410.

Fakhri M., Yousefian, F., Amoosoltani, E, Aliha, M. R. M. & Berto, F. (2021). Combined Effects of Recycled Crumb Rubber and Silica Fume on Mechanical Properties and Mode-I Fracture Toughness of Self-Compacting Concrete (SCC)" Fatigue & Fracture of Engineering Materials & Structures

Fakhri, M., Amoosoltani, E., & Aliha, M. R. M. (2017). Crack behavior analysis of roller compacted concrete mixtures containing reclaimed asphalt pavement and crumb rubber. *Engineering Fracture Mechanics, 180*, 43-59.

Guan, J.F., Li, C.M., Wang, J. (2019). Determination of fracture parameter and prediction of structural fracture using various concrete specimen types. *Theoretical and Applied Fracture Mechanics. 100*, 114–127.

Hillerborg, A., Modeer, M., & Petersson, P.E. (1976). Analysis of crack formation and crack growth in concrete by means of fracture mechanics and finite elements. *Cement & Concrete Research, 6*, 773–782.

Hou, Y.K., Duana, S.J., & An, R. M. (2019). Solving the cohesive zone model analytic function for concrete based on wedge-splitting test on a compact tension specimen. *Theoretical and Applied Fracture Mechanics, 102*, 162-170.

Hu, S., & Lu, J. (2012a). Experimental research and analysis on Double-K fracture parameters of concrete. *Advanced Science Letters, 12*(1), 192-195.

Hu, S., Mi, Z., & Lu, J. (2012b). Effect of crack-depth ratio on double-K fracture parameters of reinforced concrete. *Applied Mechanics & Materials, 226,* 937-941.

Hu, S., Zhang, X., & Xu, S. (2015). Effects of loading rates on concrete double-K fracture parameters. *Engineering Fracture Mechanics, 149*, 58-73.

Jenq, Y.S., & Shah, S.P. (1985). Two parameter fracture model for concrete. *Journal of Engineering Mechanics, ASCE, 111*(10), 1227-1241.

Karihaloo, B.L., & Nallathambi, P. (1991). Notched beam test: Mode I fracture toughness, Fracture Mechanics Test methods for concrete. Report of RILEM Technical Committee 89-FMT (Edited by S.P. Shah and A. Carpinteri), Chamman & Hall, London, 1-86.

Kumar, S., & Barai, S.V. (2008a). Influence of specimen geometry on determination of double-K fracture parameters of concrete: A comparative study. *International Journal of Fracture, 149*, 47-66.

Kumar, S., & Barai, S.V. (2008b). Cohesive crack model for the study of nonlinear fracture behaviour of concrete. *Journal of The Institution of Engineers (India), CV, 89*, 7-15.

Kumar, S., & Barai, S.V. (2009a). Determining double-K fracture parameters of concrete for compact tension and wedge splitting tests using weight function. *Engineering Fracture Mechanics, 76*, 935-948.

Kumar, S., & Barai, S.V. (2009b). Effect of softening function on the cohesive crack fracture parameters of concrete CT specimen. *Sadhana Academy Proceedings in Engineering Sciences, 36*(6), 987-1015.

Kumar, S., & Barai, S.V. (2010a). Determining the Double-K fracture parameters for three-point bending notched concrete beams using weight function. *Fatigue and Fracture of Engineering Materials and Structures, 33*(10), 645-660.

Kumar, S., & Barai, S.V. (2010b). Size-effect prediction from the double-K fracture model for notched concrete beam. *International Journal of Damage Mechanics, 19*, 473-497.

Kumar, S., & Pandey, S.R. (2012). Determination of double-K fracture parameters of concrete using split-tension cube test. *Computers and Concrete, An International Journal, 9*(1), 1-19.

Kumar, S., Pandey, S.R., & Srivastava, A.K.L. (2014). Determination of double-K fracture parameters of concrete using peak load method. *Engineering Fracture Mechanics, 131*, 471-484.

Kwon, S.H., Zhao, Z., & Shah, S.P. (2008). Effect of specimen size on fracture energy and softening curve of concrete: Part II. Inverse analysis and softening curve. *Cement and Concrete Research, 38*, 1061-1069.

Li, Y., Qing, L., Cheng, Y., Dong, M., & Ma, G. (2019). A general framework for determining fracture parameters of concrete based on fracture extreme theory. *Theoretical and applied fracture mechanics, 103* (102259), 1-16.

Murakami, Y. (1987), "Stress Intensity Factors Hand Book (Committee on Fracture Mechanics, The Society of Materials Science, Japan)", Vol-1, Pergamon Press, Oxford.

Nallathambi, P., & Karihaloo, B.L.(1986). Determination of specimen-size independent fracture toughness of plain concrete. *Magazine of Concrete Research, 38*(135), 67-76.

Pandey, S.R., Kumar. S., & Srivastava, A.K.L. (2016). Determination of double-K fracture parameters of concrete using split-tension cube: a revised procedure. *International Journal of Concrete Structures & Materials, 10*(2), 163-175.

Park, K., Paulino, G.H., & Roesler, J.R. (2008). Determination of kink point in bilinear softening model for concrete. *Engineering Fracture Mechanics, 7*, 3806-3818.

Petersson, P.E. (1981). Crack growth and development of fracture zone in plain concrete and similar materials. Report No. TVBM-100, Lund Institute of Technology.

Planas, J., & Elices, M. (1991). Non-linear fracture of cohesive material. *International Journal of Fracture, 51*, 139-157.

Pradhan, S., Kumar, S., & Barai, S.V. (2018). Impact of particle packing mix design method on fracture properties of material and recycled aggregate concrete. *Fatigue & Fracture of Engineering Materials & Structures,* 2018, 1-16.

Qing, L.B., & Li, Q.B. (2013). A theoretical method for determining initiation toughness based on experimental peak load. *Engineering Fracture Mechanics, 99*, 295-305.

Qing, L.B., Nie, Y.T., & Hu, Y.A. (2017). Simplified extreme method for determining double-K fracture parameters of concrete using experimental peak load. *Fatigue & Fracture in Engineering Materials & structures, 40*(20), 254-266.

Qinga, L., Donga, M., & Guanb, J. (2018). Determining initial fracture toughness of concrete for split-tension specimens based on the extreme theory. *Engineering Fracture Mechanics, 189*, 427-438.

Reinhardt, H.W., Cornelissen, H.A.W., & Hordijk, D.A. (1986). Tensile tests and failure analysis of concrete. *Journal of Structural Engineering, ASCE, 112*(11), 2462-2477.

Roesler, J., Paulino, G.H., Park, K., & Gaedicke, C. (2007). Concrete fracture prediction using bilinear softening. *Cement and Concrete Composites, 29*, 300-312.

Rooholamini, H., Hassani, A., & Aliha, M. R. M. (2018). Evaluating the effect of macro-synthetic fibre on the mechanical properties of roller-compacted concrete pavement using response surface methodology. *Construction and Building Materials, 159*, 517-529.

Rooholamini, H., Hassani, A., & Aliha, M. R. M. (2018). Fracture properties of hybrid fibre-reinforced roller-compacted concrete in mode I with consideration of possible kinked crack. *Construction and Building Materials, 187,* 248-256.

Ruiz, G., Ortega, José J., Yu, R.C., Xu, S., & Wu, Y. (2016). Effect of size and cohesive assumptions on the double-K fracture parameters of concrete. *Engineering Fracture Mechanics, 166*, 198-217.

Xu, S., & Reinhardt, H.W. (1998). Crack extension resistance and fracture properties of quasi-brittle materials like concrete based on the complete process of fracture. *International Journal of Fracture, 92*, 71-99.

Xu, S., & Reinhardt, H.W. (1999). Determination of double-K criterion for crack propagation in quasi-brittle materials, Part I: Experimental investigation of crack propagation. *International Journal of Fracture, 98*, 111–149.

Xu, S., & Reinhardt, H.W. (1999). Determination of double-K criterion for crack propagation in quasi-brittle materials, Part II: analytical evaluating and practical measuring methods for three-point bending notched beams. *International Journal of Fracture, 98*, 151–77.

Xu, S., & Reinhardt, H.W. (1999). Determination of double-K criterion for crack propagation in quasi-brittle materials, Part III: compact tension specimens and wedge splitting specimens. *International Journal of Fracture, 98*, 179-193.

Xu, S., & Reinhardt, H.W. (2000). A simplified method for determining double-K fracture meter parameters for three-point bending tests. *International Journal of Fracture, 104*, 181-209.

Xu, S., & Zhang, X. (2008). Determination of fracture parameters for crack propagation concrete using an energy approach. *Engineering Fracture Mechanics, 75,* 4292-4308.

Xu, S., & Zhu, Y. (2009). Experimental determination of fracture parameters for crack propagation in hardening cement paste and mortar. *International Journal of Fracture, 157*, 33-43.

Zhang, X., & Xu, S. (2011). A comparative study on five approaches to evaluate double-K fracture toughness parameters of concrete and size effect analysis. *Engineering Fracture Mechanics,78*, 2115-2138.

Zhang, X., Xu, S., & Zheng, S. (2007). Experimental measurement of double-K fracture parameters of concrete with small-size aggregates. *Frontiers in Architecture and Civil Engineering in China, 1*(4), 448-457.

Zhao, Y., & Xu, S. (2002). The influence of span/depth ratio on the double-K fracture parameters of concrete. *Journal of China Three Georges University (Natural Science), 24*(1), 35-41.

Zhao, Z., Kwon, S.H., & Shah, S.P. (2008). Effect of specimen size on fracture energy and softening curve of concrete: Part I. Experiments and fracture energy. *Cement and Concrete Research, 38,* 1049-1060.